4-2011

Systematic Studies of the Cathode-Electrolyte Interface in SOFC Cathodes Prepared by Infiltration

Rainer Küngas
University of Pennsylvania, kungas@seas.upenn.edu

John M. Vohs
University of Pennsylvania, vohs@seas.upenn.edu

Raymond J. Gorte
University of Pennsylvania, gorte@seas.upenn.edu

Suggested Citation:
R. Küngas, J.M. Vohs and R.J. Gorte. (2011). Systematic Studies of the Cathode-Electrolyte Interface in SOFC Cathodes Prepared by Infiltration. *ESC Transactions*, 35(1) 2085-2095).

Systematic Studies of the Cathode-Electrolyte Interface in SOFC Cathodes Prepared by Infiltration

Abstract
In this study, the effect of the morphology and ionic conductivity of the electrolyte material in SOFC composite cathodes is systematically studied. The specific surface area of prous yttria-stabilized zirconia (YSZ) scaffolds was varied by almost two orders of magnitude using different pore formers and surface treatment with hydrofluoric acid (HF). The effect of ionic conductivity on the performance of SOFC cathodes was studied for electrodes prepared by infiltration of 35 wt % LSF into 65% porous scandia-stabilized zirconia (ScSZ), YSZ, or yttria-alumina co-stabilized zirconia (YAZ) scaffolds of identical microstructure cathodes.

Disciplines
Biochemical and Biomolecular Engineering | Chemical Engineering | Engineering

Comments
Suggested Citation:
R. Küngas, J.M. Vohs and R.J. Gorte. (2011). Systematic Studies of the Cathode-Electrolyte Interface in SOFC Cathodes Prepared by Infiltration. *ESC Transactions*, 35(1) 2085-2095).

ECS Transactions, 35 (1) 2085-2095 (2011)
10.1149/1.3570199 ©The Electrochemical Society

Systematic Studies of the Cathode-Electrolyte Interface in SOFC Cathodes Prepared by Infiltration

R. Küngas, J. M. Vohs, and R. J. Gorte

Department of Chemical and Biomolecular Engineering, University of Pennsylvania
Philadelphia, Pennsylvania 19104, USA

In this study, the effect of the morphology and ionic conductivity of the electrolyte material in SOFC composite cathodes is systematically studied. The specific surface area of porous yttria-stabilized zirconia (YSZ) scaffolds was varied by almost two orders of magnitude using different pore formers and surface treatment with hydrofluoric acid (HF). The effect of ionic conductivity on the performance of SOFC cathodes was studied for electrodes prepared by infiltration of 35 wt % LSF into 65% porous scandia-stabilized zirconia (ScSZ), YSZ, or yttria-alumina co-stabilized zirconia (YAZ) scaffolds of identical microstructure cathodes.

Introduction

It is well known that the three-phase boundary (TPB) region accounts for most of the activity within an SOFC cathode (1). Therefore, detailed understanding of the cathode-electrolyte interface is important for designing better and more durable fuel cells.

Alternative mixed ionic and electronic conducting (MIEC) perovskites, such as LSF ($La_{1-x}Sr_xFeO_3$) or LSCF ($La_{1-x}Sr_xCo_{1-y}Fe_yO_3$) have been proposed as cathode materials for SOFCs, especially for operation at 873 – 1073 K (2-10). The ionic conductivity of LSF ($8.3\cdot10^{-4}$ S/cm at 973 K (11)) is significantly higher than that of LSM ($4\cdot10^{-8}$ S/cm at 1073 K (12)), so that oxygen adsorption and reduction do not have to be spatially confined to the TPB sites (13-15). However, the ionic conductivity of MIECs is still much lower compared to the ionic conductivity of YSZ ($1.8\cdot10^{-2}$ S/cm at 973 K (16)). Therefore, using a composite of a perovskite and YSZ can still significantly improve the performance of SOFC cathodes compared to using the perovskite alone.

The motivation of this study is to better understand the effect of electrolyte properties in such composites. Numerous studies, both experimental and theoretical, have already been conducted on this topic, but many unanswered questions remain. For example, while it has been reported that the choice of pore former can dramatically affect electrode microstructure (17-19) and that electrode microstructure plays a key role in determining SOFC performance (19), there are have been no studies thus far that establish the link between electrode specific surface area, microstructure, and electrochemical performance.

Second issue that we believe requires more rigorous investigation is the effect of the ionic conductivity of the electrolyte in SOFC composite electrodes. For example, it is commonly accepted that the substitution of YSZ in Ni-YSZ anodes with doped ceria

results in performance enhancement (20-23). However, it remains unclear whether this effect is due to the higher ionic conductivity of ceria or due to the fact that ceria possesses significant catalytic activity towards the electrode reaction (24,25). The fact that the latter may be the case is strengthened by findings by Sumi *et al.* who compared the performance of Ni-YSZ and Ni-ScSZ (scandia-doped zirconia) anodes for methane reforming. While the ionic conductivity of ScSZ is higher than YSZ, the authors found almost no improvement in performance when YSZ in the cermet was changed for ScSZ. In fact, under some conditions studied, YSZ-based cells outperformed the ScSZ-cells (26). The situation is not much clearer for SOFC composite cathodes.

Therefore, in this paper, we report the results of two systematic studies that address and clarify the issues listed above. All the measurements in this study were conducted on electrodes prepared by infiltration. However, since the performance of electrodes formed by infiltration has many similarities to that of traditional composites (27), the ideas developed here are likely to apply to traditional composites as well.

Experimental

All of the experiments in this study were performed on symmetric cells in which the electrodes were prepared by infiltration of nitrate solutions into a porous electrolyte matrix. The first step in cell fabrication involved making a porous-dense-porous electrolyte wafer using tape-casting methods. The tapes for the porous YSZ were prepared by mixing 8 mol.% YSZ powder (Tosoh) and a solvent (water or ethanol), dispersant, binders and pore formers (graphite or PMMA beads). Porous scandia-stabilized zirconia (ScSZ) and yttria-alumina co-stabilized zirconia (YAZ) scaffolds were fabricated according to the same recipe, using 10 mol.% ScSZ (Fuel Cell Materials) and 3 mol.% Y_2O_3, 20 mol.% Al_2O_3 stabilized zirconia (Tosoh) as starting materials. A detailed description of the tape-casting and lamination procedure has been given elsewhere (27-29). The resulting slurry was tape cast and laminated onto both sides of a green tape that would become the dense YSZ (or ScSZ, YAZ) electrolyte. After sintering at 1773 K for 4 hours, the resulting YSZ matrix was approximately 65-70% porous and had a surface area of 0.48 m^2/g. The microstructure of ScSZ and YAZ cells was very similar.

The HF treatment for modifying the YSZ scaffold was carried out by simply infiltrating the porous scaffold with concentrated hydrofluoric acid (MP Biomedicals) at room temperature. The solution was then left in the scaffold 1 h before being removed by washing with distilled water and ethanol.

Electrodes in this study were fabricated by infiltrating porous electrolyte scaffolds with an aqueous solution consisting of $La(NO_3)_3 \cdot 6H_2O$ (Alfa Aesar, 99.9%), $Sr(NO_3)_2$ (Alfa Aesar, 99%), and $Fe(NO_3)_3 \cdot 9H_2O$ (Fisher, 98.4%) at a molar ratio of La:Sr:Fe = 0.8:0.2:1. Citric acid, in a 1:1 ratio with the metal cations, was used as a complexing agent in order to assist the formation of the perovskite phase at lower temperatures. Infiltration steps were followed by a 0.5-h heat treatment at 723 K to decompose the nitrates. This procedure was repeated until a loading of 35-wt% LSF was achieved. The composites were then calcined to either 1123 K or to 1373 K for 4 h. For fuel-cell measurements, 45-wt% ceria and 1-wt% Pd were added to the porous layer opposite the LSF-electrolyte composite using $Ce(NO_3)_3 \cdot 6H_2O$ (Alfa Aesar, 99.5%) and tetra-ammine

palladium(II) nitrate solutions (Alfa Aesar, 99.9%), followed by calcination to 723 K followed by heat treatment at 723 K and the application of Ag current collector paste.

The fuel cells were attached to an alumina tube using a ceramic adhesive (Aremco, Ceramabond 552) so that the fuel (97% H_2-3% H_2O) could be introduced to the anode. Electrochemical impedance spectra were recorded using a Gamry Instruments potentiostat in the frequency range of 0.1 Hz to 100 kHz. All symmetric cell impedances in this paper have been divided by two to account for there being two identical electrodes. Brunauer-Emmett-Teller (BET) Kr adsorption was carried out on 3 × 3 × 10 mm slabs, prepared from the same slurries that were used in the tape-casting process.

Results

The Effect of Electrolyte Scaffold Surface Area

The samples used in this part of the study are summarized in Table 1. When graphite was used as the pore former, the specific surface area was 0.48 m^2/g. This low specific surface area demonstrates that there is no mesoporosity in the YSZ scaffold. The pore size that would be calculated for a 70% porous, YSZ scaffold with uniform cylindrical pores and this specific surface area is 2.8 μm, which is similar to the characteristic size of the channels in Fig. 1a. The specific surface area of the scaffold prepared with PMMA was much lower, 0.04 m^2/g, consistent with the much larger pores.

Table 1. Overview the properties of electrolyte samples used in this study.

Electrolyte + pore former	Specific surface area	Porosity
YSZ + graphite	0.48 m^2/g	70 %
(HF)YSZ + graphite	0.83… 3.00 m^2/g	66 %
YSZ + PMMA	0.04 m^2/g	71%

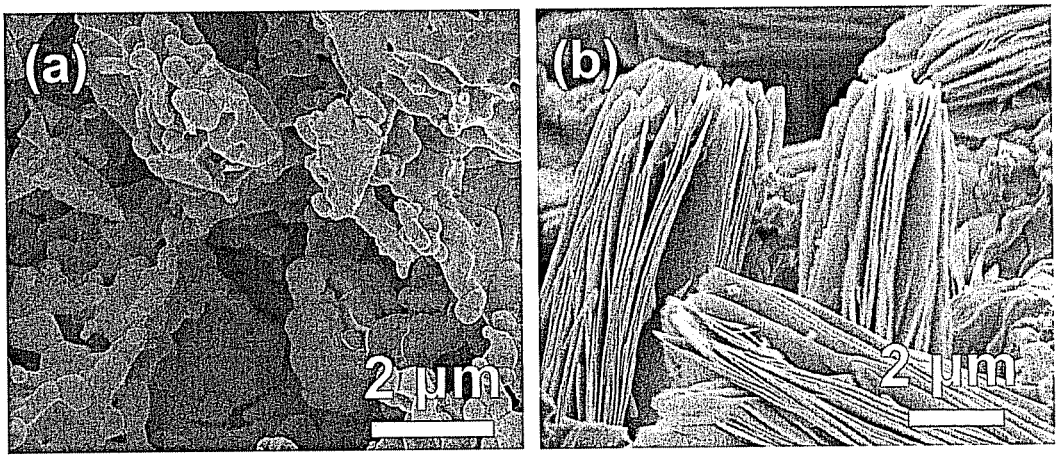

Figure 1. The microstructure of YSZ scaffolds obtained by using graphite as pore former: a) before room-temperature HF-treatment, 2) after HF-treatment.

The effect of treating the porous YSZ, made using graphite pore formers, with concentrated HF for 1 h at room temperature is shown in Fig. 1b). The sample in these images was heated in air to 823 K to remove any residual fluorine. The overall structure

remained stable but the entire pore network was changed. Sheet and pillar like structures are observed, with a characteristic length scale of less than 100 nm. HF treatment resulted in a large increase in the surface area: the specific surface area was 3.0 m^2/g right after HF-treatment, 2.1 m^2/g after 4-h heat treatment at 823 K and 0.83 m^2/g after 1373 K. The porosity of all samples was between 66-71%.

The effect of the scaffold on electrode performance is shown in Fig. 2. The data in this figure were obtained at 973 K in air on symmetric cells prepared by infiltration of 35-wt% LSF. All impedances were divided by two to account for the two identical electrodes. A comparison of the performance of the cells made with graphite-prepared YSZ, with and without HF treatment, is given in Fig. 2a). The ohmic losses, indicated by the high-frequency intercept with the real axis, were the same in both cells, 0.18 $\Omega \cdot cm^2$, and very close to half the value expected for a 75-μm YSZ electrolyte. Although the non-ohmic losses, determined from the lengths of the arcs in the Cole-Cole plot, were very good for both cells, the cell with the HF-treated scaffolds was superior, with an impedance of 0.07 $\Omega \cdot cm^2$, compared to an impedance of 0.13 $\Omega \cdot cm^2$ on the untreated cell.

While the impedance observed on the LSF-infiltrated electrode prepared with the untreated YSZ would be acceptable for most applications, previous work has shown that the impedances increase with time or increasing calcination temperature because of coarsening of the infiltrated LSF (30,31). It has been reported that heating infiltrated, LSF-YSZ composites to 1373 K had a similar effect on LSF structure as operation for several thousand hours at 973 K (31). Fig.2b) shows impedance data at 973 K from cells made by infiltration of LSF into YSZ scaffolds prepared with graphite pore formers, both HF treated and untreated, and PMMA pore formers, after calcination of the LSF to 1373 K for 4 h. The ohmic losses on all three cells were unchanged and remain the same as that expected for the YSZ electrolyte, indicating that there are no solid state reactions between LSF and YSZ; however, the effect of YSZ pore structure on the non-ohmic losses was dramatic. The impedance of the cell made with the PMMA was greater than 2 $\Omega \cdot cm^2$, while that of the graphite-prepared cells were approximately 1.2 and 0.5 $\Omega \cdot cm^2$, respectively. Clearly, this performance scaled with the surface area of the YSZ scaffold.

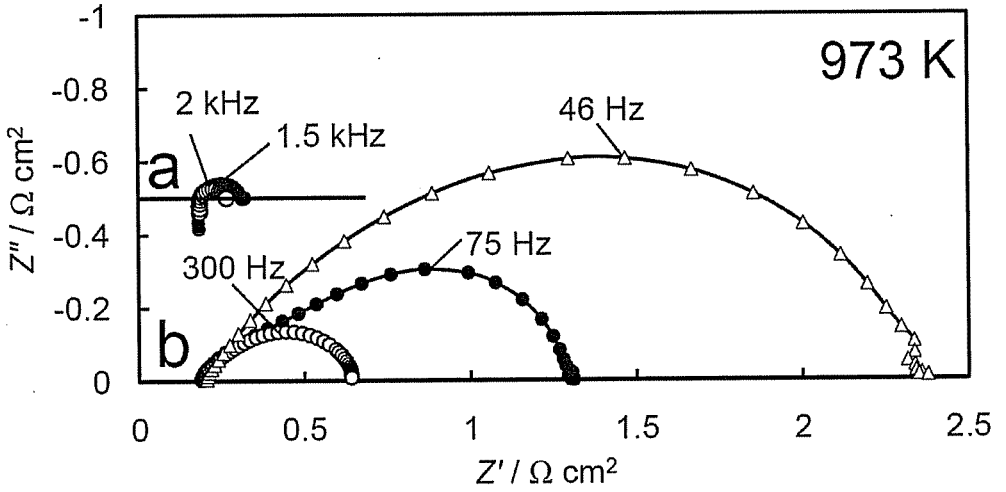

Figure 2. Electrochemical impedance spectra of LSF-YSZ symmetric cells at 973 K: a) after calcination of the composites to 1123 K, b) after calcination of the composites to 1373 K. Open circles – HF-treated YSZ, closed symbols – untreated YSZ, triangles – PMMA.

The Effect of Electrolyte Ionic Conductivity

In this study, infiltration methods were used to prepare the electrode composites because they offer a number of advantages relative to traditional fabrication methods. First, the electrolyte scaffold is calcined separately at high temperatures, prior to the addition of the perovskite, so that there is good connectivity in the electrolyte phase and no solid-state reactions between the two phases of the composite (27). Furthermore, by using tape casting with the same pore formers, the structure of the electrolyte scaffold can be identical for different electrolytes. In order to vary other materials properties of the electrolyte phase (e.g. surface energy, reducibility, chemical stability, activity as catalyst, etc.) as little as possible, we chose to compare three zirconia-based materials with very different ionic conductivities: 8 mol.% Y_2O_3-stabilized zirconia (YSZ), 10 mol.% Sc_2O_3-stabilized zirconia (ScSZ), and 3 mol.% Y_2O_3-20 mol.% Al_2O_3-doped zirconia (YAZ). The electrolyte scaffolds used in this part of the study are summarized in Table 2. We will demonstrate that the ionic conductivity of the electrolyte phase is very important in determining the cathode performance.

Table 2. Overview the properties of electrolyte samples used in this study.

Notation	**Electrolyte material**	**Ionic conductivity at 973 K**
YSZ	8 mol.% YSZ	0.0183 S/cm (16)
ScSZ	10 mol.% ScSZ	0.0280 S/cm (32)
YAZ	3 mol.% Y_2O_3, 20 mol.% Al_2O_3 stabilized ZrO_2	0.00484 S/cm (33)

The porous layers were all about 50 μm in thickness, but the thickness of the dense layers varied slightly from material to material, being 100 μm for YSZ and ScSZ, but 115 μm for YAZ. All three electrolyte scaffolds were infiltrated with an aqueous solution consisting of $La(NO_3)_3 \cdot 6H_2O$, $Sr(NO_3)_2$, $Fe(NO_3)_3 \cdot 9H_2O$ and citric acid at a molar ratio of 0.8:0.2:1:2 in order to form LSF-YSZ, LSF-ScSZ, and LSF-YAZ composite electrodes. Fig. 3a) through c) show SEM of the same structures after infiltration of LSF with calcination to 1123 K. The composites are again nearly identical in appearance, with small LSF nanoparticles (~ 50 nm in diameter) deposited on the scaffold walls. After calcination to 1373 K, Fig. 3d) through e), the LSF particles are no longer easily distinguishable from the electrolyte scaffold, appearing to form a dense film of LSF over the scaffolds. Qualitatively, there were no significant differences in the nature of the LSF particles in the three electrolyte scaffolds and the interactions between LSF and the three electrolyte materials were very similar.

Fig. 4 shows *i-V* polarization curves measured at 973 K for fuel cells made from each of the electrolytes, operating on 97% H_2-3% H_2O at the anode and air at the cathode. The LSF composites in each of the cells had been calcined to 1123 K. The open circuit voltage (OCV) was above 1.05 V in each case, close to the Nernst Potential. However, the effect of electrolyte on the maximum power densities in these three cells is large, the YAZ cell exhibiting a maximum power density of 90 mW/cm^2, the YSZ cell 280 mW/cm^2, and the ScSZ cell 790 mW/cm^2. The i-V curves were also reasonably linear, implying that the impedance of cells was nearly independent of the applied load, so that impedance spectra measured at open circuit should provide a good measure of electrode performance. Based on the average slopes of *i-V* curves, the values of overall cell

resistances were 0.36 Ω cm^2, 1.1 Ω cm^2, and 3.1 Ω cm^2 for cells based on ScSZ, YSZ, and YAZ, respectively.

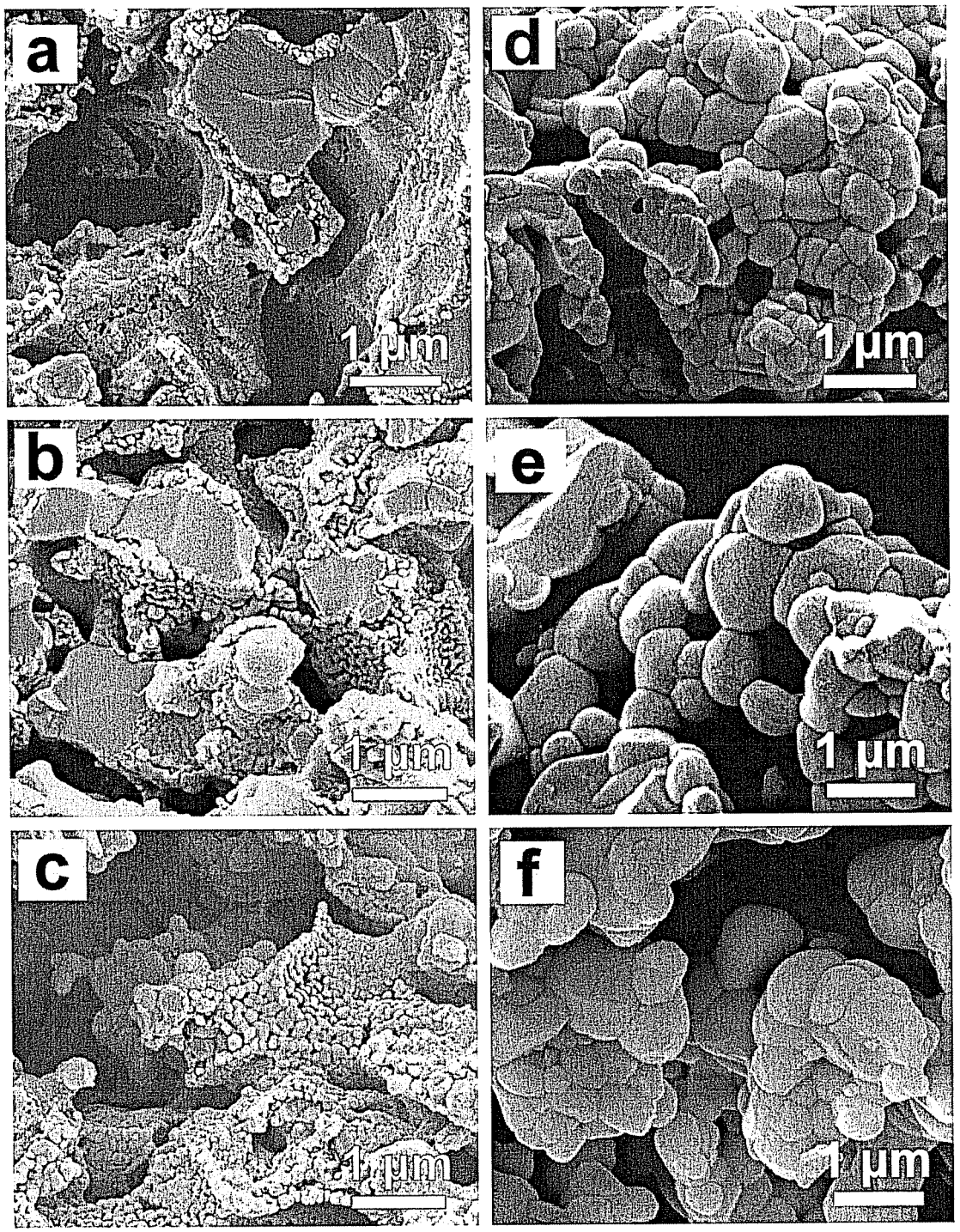

Figure 3. SEM images of porous 35-wt% LSF-SZ scaffolds: (a),(b) LSF-ScSZ, (c),(d) LSF-YSZ, and (e),(f) LSF-YASZ. Samples shown in (a),(c), and (e) were calcined to 1123 K, whereas samples (b),(d), and (f) were calcined to 1373 K.

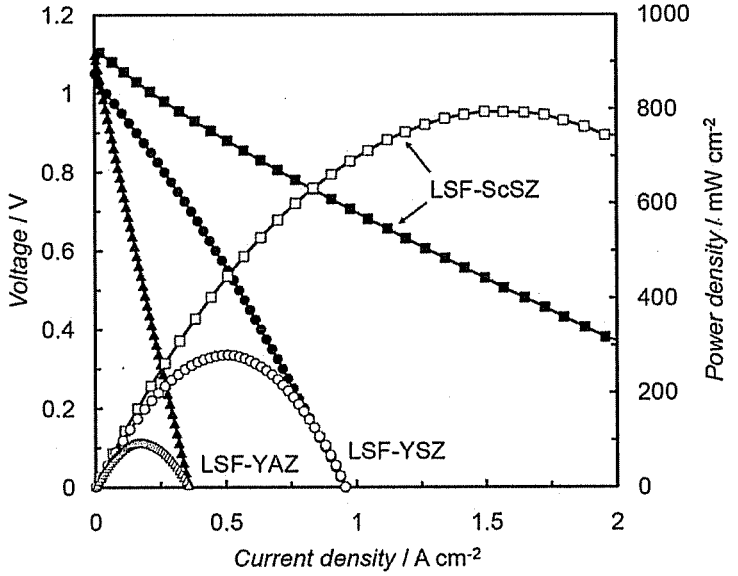

Figure 4. Polarization i-V curves for of LSF-SZ-LSCM,CeO_2,Pd fuel cell single cells with different electrolyte scaffolds after calcination to 1123 K, measured at 973 K. The cathode was subject to ambient air whereas 3% humidified H_2 was pumped onto the anode side. Closed symbols – voltage, open symbols – power density.

The corresponding open-circuit impedance spectra for the three cells were collected in order to separate the electrode losses from the ohmic losses. Based on the impedance spectra, the total cell resistances, were 0.28 $\Omega \cdot cm^2$ for the ScSZ cell, 0.84 $\Omega \cdot cm^2$ for the YSZ cell, and 3.12 $\Omega \cdot cm^2$ for the YAZ cell. The electrolyte losses, calculated from the high-frequency intercept with the real axis in the impedance spectra, were a large fraction of the losses in each cell. At 973 K, the ohmic contributions to the cells were 0.22 $\Omega \cdot cm^2$ for the ScSZ cell, 0.51 $\Omega \cdot cm^2$ for the YSZ cell, and 2.37 $\Omega \cdot cm^2$ for the YAZ cell. When these losses are subtracted off from the total cell losses, the polarization losses associated with the electrodes is obtained, 0.06 $\Omega \cdot cm^2$, 0.33 $\Omega \cdot cm^2$, and 1.16 $\Omega \cdot cm^2$ for LSF composites with ScSZ, YSZ, and YAZ, respectively

Since the ionic conductivity, σ_i, is related to the ohmic resistance, R_Ω, and the thickness of the electrolyte, l, by $\sigma_i = l / R_\Omega$, we calculated the values of R_Ω corresponding to 100 μm YSZ, 100 μm ScSZ, and 115 μm YAZ from the conductivity data provided in Table 2. The resulting R_Ω values of 0.36 $\Omega \cdot cm^2$, 0.54 $\Omega \cdot cm^2$, and 2.38 $\Omega \cdot cm^2$, for ScSZ, YSZ, and YAZ, respectively, are in good agreement with our experimental values.

Importantly, the impedance data indicate that electrode losses depend strongly on the ionic conductivity of the electrolyte scaffold. However, because there are contributions from both the anode and cathode in these measurements, it is difficult to quantify the effect of the electrolyte. In order to isolate the effect of varying the electrolyte material on the electrochemical activity of the composite cathodes, symmetric cells were prepared in which LSF was infiltrated into both sides of the porous-dense-porous, stabilized-zirconia structures. Impedance spectra were then measured in air over the temperature range from 873 to 973 K, the spectra obtained at 973 K shown in Fig. 5a for cells in which the LSF was calcined at 1123 K. The ohmic losses have been subtracted from the Cole-Cole plots and the values divided by two to account for the there being two electrodes. In agreement

with the fuel cell data, the polarization resistances, R_p, increased with decreasing conductivity, with R_p being the smallest for ScSZ and the largest for YAZ.

Because the performance of infiltrated electrodes depends on the calcination temperature (30,31,34), symmetric cells were also prepared with the LSF calcined to 1373 K for 4 h. Impedance spectra were again obtained in air from 873 to 973 K, with the spectra at 973 K shown in Fig. 5b. Although the impedances on each of these cells were significantly higher, the relative performance as a function of the electrolyte was the same, with the ScSZ cell being the best with an R_p of 0.54 Ω cm^2, while the YSZ and YAZ cells showed significantly higher R_p of 0.91 Ω cm^2 and 2.67 Ω cm^2, respectively.

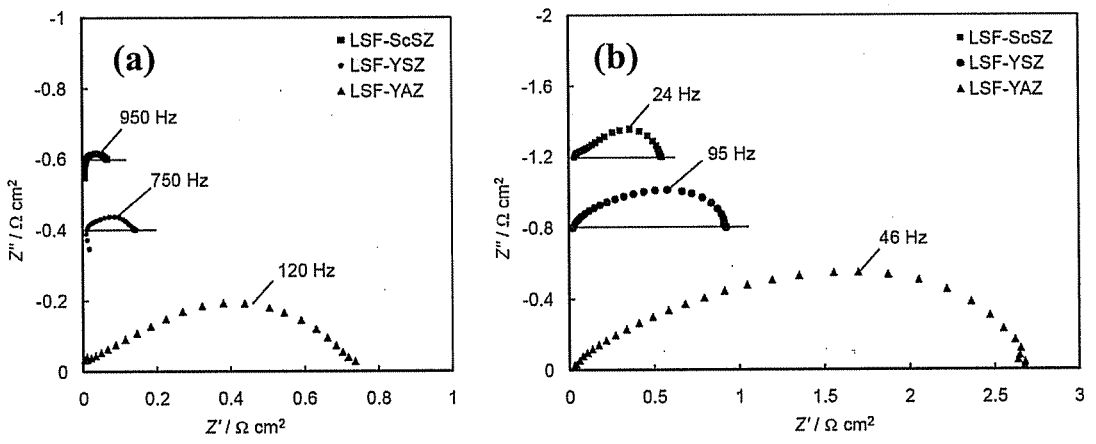

Figure 5. Electrochemical impedance spectra of LSF-YSZ symmetric cells with different electrolyte scaffolds after calcination to a) 1123 K and b) 1373 K, measured at 973 K in ambient air and open circuit conditions. Squares – ScSZ, circles – YSZ, triangles –YAZ.

Discussion

Both the surface area of the electrolyte and the ionic conductivity play an important role in determining the electrochemical activity of SOFC composite cathodes.

Closer examination reveals that the dependence on the surface area of the electrolyte is fairly strong: for the LSF-(PMMA)YSZ, LSF-YSZ, and LSF-(HF)YSZ symmetric cells calcined to 1373 K, the resistance is an inverse square function of the scaffold surface area. Unfortunately, increasing the surface area of a YSZ scaffold that is calcined at 1773 K is not a trivial task. We believe that it is very difficult to obtain surface areas > 1 m^2/g using approach that involves carbonaceous pore formers only. Other routes, such as the use of inorganic pore formers (35), metathesis (36), or surface treatments with etching agents (such as the HF-treatment proposed here) is necessary and even then, degradation of the scaffold structure may occur.

We have also shown that the polarization resistance of composite electrodes decreases as the ionic conductivity of the electrolyte used in the composite increases, when all other materials properties (such as the catalytic activity, microstructure, reducibility, surface energy, etc.) are held constant. In contrast to doped ceria, none of the three electrolyte materials in this study is likely to possess significant activity towards

oxygen reduction reaction, thus eliminating the possibility of electrode performance enhancement due to catalytic activity.

Modeling studies by Tanner *et al.* have predicted that the polarization resistance of composite cathode should vary as the inverse square-root of the ionic conductivity of the electrolyte material (13). In our study, we did observe weaker-than-linear log-log slopes for plots of polarization resistance vs ionic conductivity for 'deactivated' cells (i.e. cells heated to 1373 K, Fig. 5b): e.g. -0.73 at 973 K and -0.48 at 923 K. However, for cells calcined to 1123 K (Fig. 5a), the dependence was almost perfectly linear at 973 K.

One implication of the finding that the performance scales with the ionic conductivity is that at least some of the enhancement observed when substituting YSZ with doped ceria in electrode composites arises from the increased ionic conductivity of the doped ceria. Of course, using a ceria-based composite can be advantageous in other ways. For example, doped ceria can prevent solid state reactions between YSZ and LSCo ($La_{1-x}Sr_xCoO_3$) (34,37). Ceria could also enhance performance through enhanced catalytic activity, since it is known to be a very good oxidation catalyst (24,25).

Another implication of our results is related to low-temperature SOFCs. ScSZ is often proposed as a promising electrolyte material for anode-supported thin-electrolyte fuel cells operating at temperatures below 873 K (38,39). The results of the present study demonstrate that a significant fraction of the enhanced performance of cells based on ScSZ could be due to enhanced performance of composite electrodes made from ScSZ. For very thin electrolytes, electrode losses frequently dominate. Improved ionic conductivity of the electrolyte within the composite electrodes could still affect the overall cell performance.

While all of the data in the present study was taken on composites of LSF and the electrolyte material, it is likely that the conclusions will be general for any perovskite so long as its ionic conductivity is less than that of the electrolyte. If electronically conductive materials could be found with ionic conductivities that were higher than that of the electrolyte, there would be no need for ionic conduction within the electrolyte phase. A corollary of this is that one should expect that enhanced electrode performance following the addition of any material with high ionic conductivity to a composite cathode. Obviously, the structure of the composite is still important and one can only take advantage of a materials ionic conductivity if it is possible for that material to transport ions to the electrolyte (30).

Conclusion

Both the surface area of the electrolyte and the ionic conductivity play an important role in determining the electrochemical activity of SOFC composite cathodes. More specifically, we have shown that the polarization resistance of composite electrodes decreases as the surface area of the underlying electrolyte scaffold increases, as well as when the ionic conductivity of the electrolyte scaffold increases.

Acknowledgments

This work was funded by the U.S. Department of Energy's Hydrogen Fuel Initiative (Grant no. DE-FG02-05ER15721). We also thank the U. S. National Science Foundation's MRSEC program, grant no. DMR05-20020, for the use of the SEM.

References

1. S. Singhal and K. Kendall, *High temperature solid oxide fuel cells: fundamentals, design and applications*, Elsevier, Oxford (2003).
2. S. P. Simner, J. F. Bonnett, N. L. Canfield, K. D. Meinhardt, J. P. Shelton, V. L. Sprenkle, and J. W. Stevenson, *J. Power Sources,* **113**, 1 (2003).
3. M. Søgaard, P. V. Hendriksen, and M. Mogensen, *J. Solid State Chem.,* **180**, 1489 (2007).
4. J. Mizusaki, M. Yoshihiro, S. Yamauchi, and K. Fueki, *J. Solid State Chem.,* **58**, 257 (1985).
5. Y. Huang, J. M. Vohs, and R. J. Gorte, *J. Electrochem. Soc.*, **151**, A646 (2004).
6. Z. Lu, J. Hardy, J. Templeton, J. Stevenson, *J. of Power Sources,* **196**, 39 (2011).
7. W. G. Wang and M. Mogensen, *Solid State Ionics,* **176**, 457 (2005).
8. A. Mai, V. A. C. Haanappel, S. Uhlenbruck, F. Tietz, and D. Stöver, *Solid State Ionics*, **176**, 1341 (2005).
9. J. M. Serra, V. B. Vert, M. Betz, V. A. C. Haanappel, W. A. Meulenberg, and F. Tietz, *J. Electrochem. Soc.*, **155**, B207 (2008).
10. M. Shah and S.A. Barnett, *Solid State Ionics,* **179**, 2059 (2008).
11. F. Bidrawn, S. Lee, J. M. Vohs R. J. Gorte, *J. Electrochem. Soc.*, **155**, B660 (2008).
12. Y. Ji, J. A. Kilner and M. F. Carolan, *Solid State Ionics*, **176**, 937 (2005).
13. C. W. Tanner, K.-Z. Fung, A. V. Virkar, *J. Electrochem. Soc.*, **144**, 21 (1997).
14. E. Ivers-Tiffée, A. Weber, D. Herbstritt, *J. Eur. Ceram. Soc.,* **21**, 1805 (2001).
15. S. B. Adler, J. A. Lane, B. C. H. Steele, *J. Electrochem. Soc.*, **143**, 3554 (1996).
16. V. V. Kharton, F.M.B. Marques, A. Atkinson, *Solid State Ionics* **174**, 135 (2004).
17. S. F. Corbin and P. S. Apté, *J. Am. Ceram. Soc.*, **82**, 1693 (1999).
18. A. Sanson, P. Pinasco, and E. Roncari, *J. Eur. Ceram. Soc.* **28**, 1221 (2008).
19. Y. Y. Huang, K. Ahn, J. M. Vohs, and R. J. Gorte, *J. Electrochem. Soc.*, **151**, A1592 (2004).
20. A. Atkinson, S. Barnett, R. J. Gorte, J. T. S. Irvine, A. J. McEvoy, M. Mogensen, S. C. Singhal, and J. Vohs, *Nature Materials*, **3**, 17 (2004).
21. H. Timmermann, D. Fouquet, A.Weber, E. Ivers-Tiffée, U. Hennings, and R. Reimert, *Fuel Cells*, **6**, 307 (2006).
22. M. Cimenti, V. Alzate-Restrepo, J. M. Hill, *J. Power Sources*, **195**, 4002 (2010).
23. C. Lu, S. An, W.L. Worrell, J.M. Vohs, and R.J. Gorte, *Solid State Ionics,* **175**, 47 (2004).
24. A. Trovarelli, *Catalysis by Ceria and Related Materials*, Imperial College Press, London (2002).
25. R. J. Gorte, *AIChE Journal*, **56** 1126 (2010).
26. H. Sumi, K. Ukai, Y. Mizutani, H. Mori, C.-J. Wen, H. Takahashi, and O. Yamamoto, *Solid State Ionics*, **174**, 151 (2004).
27. J. M. Vohs and R. J. Gorte, *Advanced Materials*, **21**, 943 (2009).
28. R. Küngas, J.-S. Kim, J. M. Vohs, and R. J. Gorte, *J. Am. Ceram. Soc.*, accepted.

29. R. Küngas, J. M. Vohs, and R. J. Gorte, *J. Electrochem. Soc.*, submitted.
30. F. Bidrawn, G. Kim, N. Aramrueang, J. M. Vohs, and R. J. Gorte, *J. Power Sources*, **195**, 720 (2010).
31. W. S. Wang, M. D. Gross, J. M. Vohs, and R. J. Gorte, *J. Electrochem. Soc.*, **154**, B439 (2007).
32. J. H. Joo and G. M. Choi, *Solid State Ionics*, **179**, 1209 (2008).
33. O. Yamamoto, T. Kawahara, K. Kohno, Y. Takeda, and N. Imanashi, in *Solid State Materials*, S. Radhakrishna and A. Daud, Editors, p. 372, Narosa Publishing House, New Delhi (1991).
34. R. Küngas, F. Bidrawn, J. M. Vohs, and R. J. Gorte, *Electrochem. Solid-State Lett.*, **13**, B87 (2010).
35. M. Boaro, J. M. Vohs and R. J. Gorte, *J. Am. Ceram. Soc.*, **86**, 395 (2003).
36. E. S. Toberer, J. C. Weaver, K. Ramesha, and R. Seshadri, *Chem. Mater.* **16**, 2194, (2004)
37. S. Uhlenbruck, T. Moskalewicz, N. Jordan, H.-J. Penkalla, and H. P. Buchkremer, *Solid State Ionics*, **180**, 418 (2009).
38. T. Suzuki, Z. Hasan, Y. Funahashi, T. Yamaguchi, Y. Fujishiro, and M. Awano, *Science*, **325**, 852 (2009).
39. K. Yamahara, C. P. Jacobson, S. J. Visco, L. C. De Jonghe, *Solid State Ionics,* **176**, 275 (2005).